Supporting Information for:

Further Characterization of Cys-Type and Ser-Type Anaerobic Sulfatase Maturating Enzymes Suggests a Commonality in Mechanism of Catalysis

Tyler L. Grove[‡], Jessica H. Ahlum[‡], Rosie M. Qin[§], Nicholas D. Lanz[§], Matthew I. Radle[‡], Carsten Krebs[‡,§], and Squire J. Booker*[‡,§]*

Figure S1. Sequence alignment of anSMEcpe cloned from *C. perfring*ens (ATCC #13124D-5) and the gene from *C. perfringens* strain 13 (accession #BAB80341). Differences between the sequence determined herein and the sequence in the database are highlighted in red.

Figure S2. EPR of M□ssbauer samples. anSMEcpe AI (red trace), anSMEcpe RCN (black trace), anSMEcpe$_{C15A/C19A/C22A}$ AI (green trace), and anSMEcpe$_{C15A/C19A/C22A}$ RCN (blue trace). Spectra were collected on a Bruker ESP-300 X-Band EPR spectrometer with the following parameters: frequency, 9.51 GHz; temperature, 13 K; power, 0.101 mW; and modulation amplitude, 10 Gauss. Spin quantification was performed by comparing the double integral of the obtained signal to that of a 1 mM Cu(II)-EDTA standard collected under identical conditions.

Figure S3. LC-MS analysis of anSMEcpe assay. The assay was conducted as described in Materials and Methods using **Kp18Cys** as the substrate, **Kp9Ser** as an internal standard, and dithionite (4.5 mM) as the required reductant. Green (t=0); Red (t=30 min); Black (t=5, 10, and 20 min).

Figure S4. Turnover of WT RCN anSMEcpe with **Cp18Cys**. **A)** Time-dependent formation of 5'-dA (black triangles) and depletion of **Cp18Cys (red squares)** in the presence of dithionite. Reaction mixtures contained 4 μM anSMEcpe, 1 mM SAM, 1 mM **Cp18Cys,** and 3 mM dithionite. The data are the averages of two independent trials, and error bars denote one standard deviation. $V_{max}/[E_T]$ values for 5'-dA formation and peptide consumption are 4.50 ± 0.052 min^{-1} and 1.91 ± 0.259 min^{-1}, respectively. **B)** Time-dependent formation of 5'-dA (black triangles) and depletion of **Cp18Cys (red squares)** in the presence of the Flv/Flx/NADPH reducing system. Reaction mixtures contained 40 μM anSMEcpe, 1 mM SAM, 1 mM **Cp18Cys,** 50 μM Flv, 15 μM Flx, and 2 mM NADPH. The data are the averages of two independent trials, and error bars denote one standard deviation. $V_{max}/[E_T]$ values for 5'-dA formation and peptide consumption are 0.22 ± 0.003 min^{-1} and 0.21 ± 0.032 min^{-1}, respectively.

Figure S5. Time-dependent formation of 5′-dA (black triangles) and **Kp18FGly** (red squares) in the presence of Kp18SeCys. Reaction mixtures contained 40 μM anSMEcpe, 1 mM SAM, 0.5 mM **Kp18SeCys,** 50 μM Flv, 15 μM Flx, and 2 mM NADPH. $V_{max}/[E_T]$ values for 5'-dA and **Kp18FGly** formation are 0.053 min^{-1} and 0.032, respectively.

Figure S6. Low-temperature X-Band EPR of Flv• and anSMEcpe during turnover. Reaction mixtures contained 100 μM anSMEcpe, 2 mM SAM, 2 mM **Kp18Cys** and 204 μM Flv• (ε_{580}=4.57 mM^{-1} cm^{-1}) at 13 K at 1 min (green), 15 min (red), and 30 min (black). Spectra were collected on a Bruker ESP-300 X-Band EPR spectrometer under the following conditions:

frequency, 9.51 GHz; temperature, 13 K; power, 0.101 mW; and modulation amplitude, 10 Gauss.

Figure S7. Correlation of spectral changes and product formation during AtsB turnover with **Kp18Cys**. **A**) X-Band EPR (77 K) spectra of a reaction mixture containing 150 μM AtsB, 1 mM SAM, 1 mM **Kp18Ser,** 75 μM Flv_{ox}, and 75 μM Flv• at 1 min (red), 15 min (green), and 30 min (black). Spectra were recorded as described in Materials and Methods. **B**) Time-dependent quantification of Flv• (open circles) and 5′-dA (closed triangles). The black line is a fit of the 5'-dA data to an equation describing a burst phase followed by a steady-state linear phase.

Figure S8. Stereochemical designation of threonine and *allo*-threonine.

Figure S9. MALDI MS analysis of a WT RCN anSMEcpe reaction with **Kp18Thr** (**A**), or **Kp18*allo*Thr** (**B**). Aliquots removed from the reaction at 0 min (black trace) and 10 min (red trace) were derivatized with DNPH as described in Materials and Methods. Spectra were recorded as previously described [(1)].

Figure S10. MALDI MS analysis of a WT RCN AtsB reaction with **Kp18Thr** (**A**), or **Kp18*allo*Thr** (**B**). Aliquots removed from the reaction at 0 min (black trace) and 10 min (red trace) were derivatized with DNPH as described in Materials and Methods. Spectra were recorded as previously described [(1)].

Figure S11. UV-vis spectra of AI AtsB C127A and C245A. AI AtsB C127A (11.3 μM; solid black trace, left axis) contained 9.8 ± 0.1 irons and 9.6 ± 0.5 sulfides per polypeptide. AI AtsB C245A variant (6.2 μM; dashed red trace, right axis) contained 12.0 ± 1.1 irons and 15.0 ± 0.3 sulfides per polypeptide. The A_{395}/A_{280} ratio for both is 0.38.

Figure S12. UV-vis spectrum of AI AtsB C291A. The protein (6.4 μM), contained 6.7 ± 0.1 irons and 5.6 ± 0.6 sulfides per polypeptide. The A_{405}/A_{280} ratio was 0.39.

Figure S13. UV-vis spectrum of AI (solid line) and RCN (dashed line) anSMEcpe C276A. AI anSMEcpe C276A (4 μM, solid line, left *Y*-axis) and RCnN anSMEcpe C276A (8.4 μM, dotted line, right *Y*-axis). The A_{410}/A_{280} ratios of AI and RCN proteins were 0.36 and 0.45, respectively.

Figure S14. UV-vis of Flv• added to electron counting reaction with anSMEcpe.

Table S1: List of primers for site-directed mutagenesis of AtsB

Primer	Sequence
AtsB C127A Forward	5’-gctgatcaacgacgcatgg**GCC**cgactgttccgcg-3’
AtsB C127A Reverse	5’-cgcggaacagtcg**GGC**ccatgcgtcgttgatcagc-3’
AtsB C245A Forward	5’-ggcggaagcgc**GCC**gatagagggcg-3’
AtsB C245A Reverse	5’-cgccctctatc**GGC**gcgcttccgcc-3’
AtsB C270A Forward	5’-ccagcggcagc**GCC**gtgcacagcg-3’
AtsB C270A Reverse	5’-cgctgtgcac**GGC**gctgccgctgg-3’
AtsB C276A Forward	5’-cgtgcacagcgcccgc**GCC**ggcagcaacctgg-3’
AtsB C276S Reverse	5’-ccaggttgctgcc**GGC**gcgggcgctgtgcacg-3’
AtsB C276S Forward	5’-cgtgcacagcgcccgc**TCC**ggcagcaacctgg-3’
AtsB C276A Reverse	5’-ccaggttgctgcc**GGA**gcgggcgctgtgcacg-3’
AtsB C291A Forward	5’-ggacagctctacgcc**GCC**gaccacctgatcaacg-3’
AtsB C291A Reverse	5’-cgttgatcaggtggtc**GGC**ggcgtagagctgtcc-3’
AtsB C331A Forward	5’-gcgccgcgaa**GCC**cagacttgctcgg-3’
AtsB C331A Reverse	5’-ccgagcaagtctg**GGC**ttcgcggcgc-3’
AtsB C334A Forward	5’-ccgcgaatgccagact**GCC**tcggtaaaaatgg-3’
AtsB C334A Reverse	5’-ccatttttaccga**GGC**agtctggcattcgcgg-3’
AtsB C340A Forward	5’-cggtaaaaatggtc**GCC**cagggcggctgccc-3’
AtsB C340A Reverse	5’-gggcagccgccctg**GGC**gaccatttttaccg-3’
AtsB C344A Forward	5’-ggtctgccagggcggc**GCC**ccggcgcatctcaacgccg-3’
AtsB C344A Reverse	5’-cggcgttgagatgcgccgg**GGC**gccgccctggcagacc-3’
AtsB C357A Forward	5’-ggcaacaaccgcctc**GCC**ggaggctactaccgc-3’
AtsB C357A Reverse	5’-gcggtagtagcctcc**GGC**gaggcggttgttgcc-3’
anSMEcpe C276 Forward	5’-ggagtgtttatcctGCTgatttttatgttttagataaatgg-3’
anSMEcpe C276 Reverse	5’-ccatttatctaaaacataaaaatcAGCaggataaacactcc-3’

Table S2: Retention times and monitored *m/z* values for Detection Method 1

	Retention Time	Parent Ion*	Product Ion 1†	Product Ion 2†
5'-dA	4.7 min	252.1 (90)	136 (13)	119 (50)
Tryptophan (IS)	6.2 min	188 (130)	146.1 (10)	118 (21)

*Respective fragmentor voltages are in parenthesis.

†Respective collision energies are in parenthesis.

Table S3: Retention times and monitored *m/z* values for Detection Method 2

Substrate	Retention Time	Parent Ion*	Product Ion 1†	Product Ion 2†
Kp9Ser (IS)	1.4 min	474.4 (180)	719.3 (15)	561.3 (11)
Kp18FGly	3.9 min	1000.7 (180)	905.9 (12)	404.2 (20)
Kp18Ser	4.0 min	1001.7 (180)	906.9 (12)	404.2 (12)
Kp18Cys	4.4 min	1009.9 (180)	1727.8 (12)	914.9 (12)
Kp18SeCys	4.8 min	1033.1 (180)	1414.6 (0)	291.1 (24)
Cp18Cys	4.8 min	955.3 (180)	477.2 (16)	421.2 (8)
Kp18Thr	4.1 min	1008.7 (180)	1059.6 (18)	914 (14)
Kp18*allo*Thr	3.9 min	1008.7 (180)	1059.6 (18)	914 (14)

*Respective fragmentor voltages are in parenthesis.

†Respective collision energies are in parenthesis.

Figure S1

```
AnSMEcpe  1    ATGCCACCATTAAGTTTGCTTATTAAGCCAGCTTCTAGTGG 41
BAB80341  1    ATGCCACCATTAAGTTTGCTTATTAAGCCAGCTTCTAGTGG 41

AnSMEcpe  42   ATGTAATTTAAAATGCACTTATTGTTTTTATCATTCTTTAA 82
BAB80341  42   ATGTAATTTAAAATGCACTTATTGTTTTTATCATTCTTTAA 82

AnSMEcpe  83   GTGATAATAGAAATGTTAAGAGCTACGGAATTATGAGAGAT 123
BAB8034   83   GTGATAATAGAAATGTTAAGAGCTATGGAATTATGAGAGAT 123

AnSMEcpe  124  GAAGTTTTAGAAAGCATGGTCAAAAGGGTTTTGAATGAAGC 164
BAB8034   124  GAAGTTTTAGAAAGCATGGTTAAAAGGGTTTTGAATGAAGC 164

AnSMEcpe  165  TAATGGACATTGCAGTTTTGCTTTTCAGGGAGGAGAACCTA 205
BAB80341  165  TGATGGCCATTGTAGTTTTGCTTTTCAGGGAGGAGAACCTA 205

AnSMEcpe  206  CCTTAGCAGGATTAGAATTTTTTGAAAAGTTAATGGAGCTT 246
BAB80341  206  TCTTAGCAGGATTAGAATTTTTTGAAAGGTTAATGGAGCTT 246

AnSMEcpe  247  CAGAGAAAACATAATTATAAAAATTTAAAAATATATAATAG 287
BAB80341  247  CAGAGGAAACATAATTATAAAAATTTAAAAATATATAATAG 287

AnSMEcpe  288  TTTGCAAACCAATGGAACTTTAATAGATGAAAGTTGGGCAA 328
BAB80341  288  TTTGCAAACCAATGGAACTTTAATAGATGAAAGTTGGGCAA 328

AnSMEcpe  329  AGTTTTTAAGTGAAAATAAATTTCTTGTGGGACTATCTATG 369
BAB80341  329  AGTTTTTAAGTGAAAATAAATTTCTTGTGGGACTATCTATG 369

AnSMEcpe  370  GATGGACCTAAGGAAATACACAATTTAAATAGAAAAGATTG 410
BAB80341  370  GATGGACCTAAGGAAATACACAATTTAAATAGAAAAGATTG 410

AnSMEcpe  411  TTGTGGTTTAGATACCTTTAGTAAGGTAGAAAGGGCAGCGG 451
BAB80341  411  TTGTGGTTTAGATACCTTTAGTAAGGTAGAAAGGGCAGCGG 451

AnSMEcpe  452  AGTTATTTAAAAAGTATAAGGTTGAATTTAATATATTATGC 492
BAB80341  452  AGTTATTTAAAAAGTATAAGGTTGAATTTAATATATTATGC 492

AnSMEcpe  493  GTTGTGACCTCTAATACAGCTAGGCATGTAAATAAAGTATA 533
BAB80341  493  GTTGTGACCTCTAATACAGCTAGGCATGTAAATAAAATATA 533

AnSMEcpe  534  TAAATATTTTAAGGAAAAAGATTTTAAATTTCTTCAATTTA 574
BAB80341  534  TAGATATTTTAAGGAAAAAGATTTTAAATTTCTTCAATTTA 574

AnSMEcpe  575  TAAATTGTCTTGACCCATTGTACGAGGAAAAAGGTAAATAT 615
BAB80341  575  TAAATTGTCTTGACCCATTGTACGAGGAAAAGGGTAAATAT 615

AnSMEcpe  616  AATTATTCTTTAAAGCCAAAGGATTATACTAAGTTTTTAAA 656
BAB80341  616  AATTATTCTTTAAAACCACAGGATTATACTAAGTTTTTAAA 656

AnSMEcpe  657  GAATTTATTCGACTTTTGGTATGAAGATTTTCTAAATGGAA 697
BAB80341  657  GAATTTATTTGACTTGTGGTATGAAGATTTTCTAAATGGAA 697

AnSMEcpe  698  ATAGAGTAAGCATTAGATATTTTGATGGTTTATTAGAAACA 738
```

```
BAB80341  698  ATAGAGTAAGCATTAGATATTTTGATGGTTTACTAGAAACA 738

AnSMEcpe  739  ATTTTATTAGGAAAGTCATCATCTTGTGGAATGAATGGGAC 779
BAB80341  739  ATTTTATTAGGAAAGTCATCATCTTGTGGAATGAATGGGAC 779

AnSMEcpe  780  ATGTACCTGTCAGTTTGTTGTGGAAAGTGATGGGAGTGTTT 820
BAB80341  780  ATGTACCTGTCAGTTTGTTGTGGAAAGTGATGGGAGTGTTT 820

AnSMEcpe  821  ATCCTTGTGATTTTTATGTTTTAGATAAATGGAGACTAGGC 861
BAB80341  821  ATCCTTGTGATTTTTATGTTTTAGATAAATGGAGACTAGGC 861

AnSMEcpe  862  AACATACAGGATATGACAATGAAAGAATTATTTGAAACCAA 902
BAB80341  862  AACATACAGGATATGACAATGAAAGAATTATTTGAAACAAA 902

AnSMEcpe  903  TAAAAATCATGAGTTTATAAAATTATCATTTAAAGTTCATG 943
BAB80341  903  TAAAAATCATGAGTTTATAAAATCATCCTTTAAAGTTCATG 943

AnSMEcpe  944  AAGAATGCAAAAAGTGCAAGTGGTTTAGACTTTGTAAAGGT 984
BAB80341  944  AAGAATGTAAAAAGTGCAAGTGGTTTAAGCTTTGTAAAGGT 984

AnSMEcpe  985  GGATGTAGAAGGTGCAGAGATTCAAAGGAAGATTCAGCTTT 1025
BAB80341  985  GGATGTAGAAGGTGCAGAGATTCAAAGGAAGACTCAGACTT 1025

AnSMEcpe  1026 AGAGTTAAACTACTATTGTCAAAGCTACAAGGAATTCTTTG 1066
BAB80341  1026 AGAGTTAAACTACTATTGCCAAAGTTACAAGGAATTCTTTG 1066

AnSMEcpe  1067 AATATGCCTTTCCAAGGTTAATAAATGTTGCCAACAATATT 1107
BAB80341  1067 AATATGCCTTTCCAAGGTTAATAAATGTTGCCAACAATATT 1107

AnSMEcpe  1108 AAATCGGATCCGAATTCGAGCTCCGTCGACAAGCTTGCGGC 1148
BAB80341  1108 AAATAA                                  1113

AnSMEcpe  1149 CGCACTCGAGCACCACCACCACCACTGAGATCCGGCTG 1189
BAB80341  1114                                      1113

AnSMEcpe  1190 CTAACAAAGCCCGAA 1204
BAB80341  1114               1113
```

Figure S2

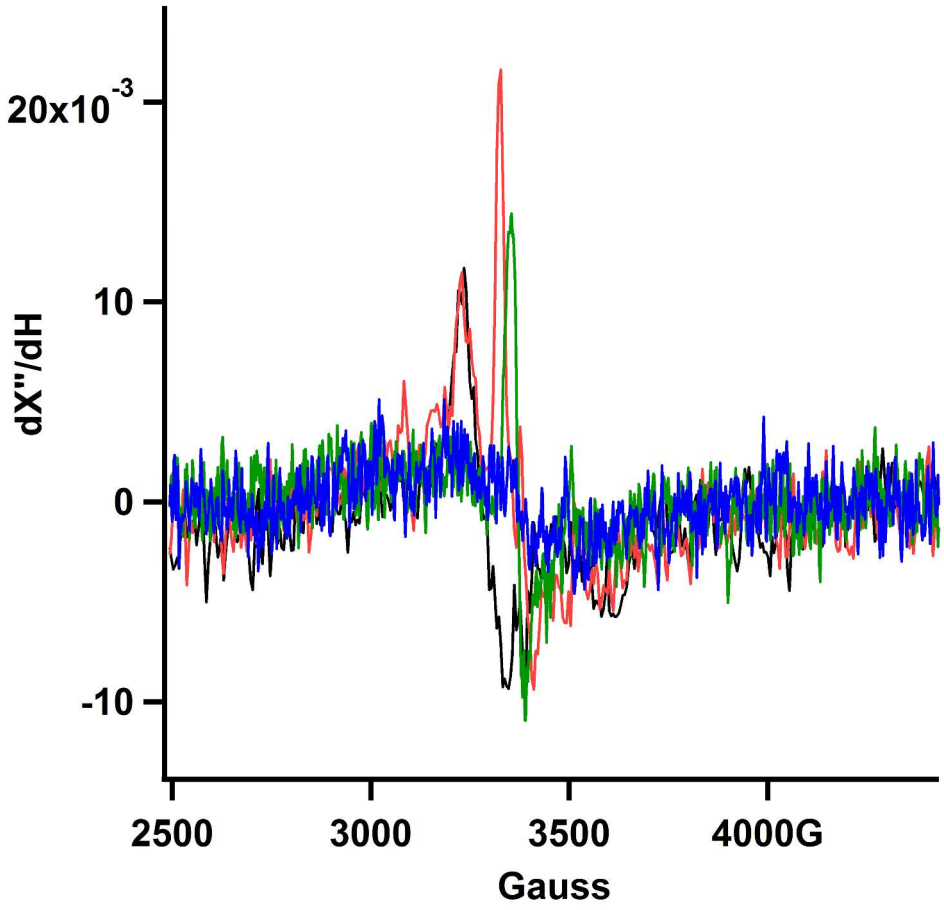

Figure S3

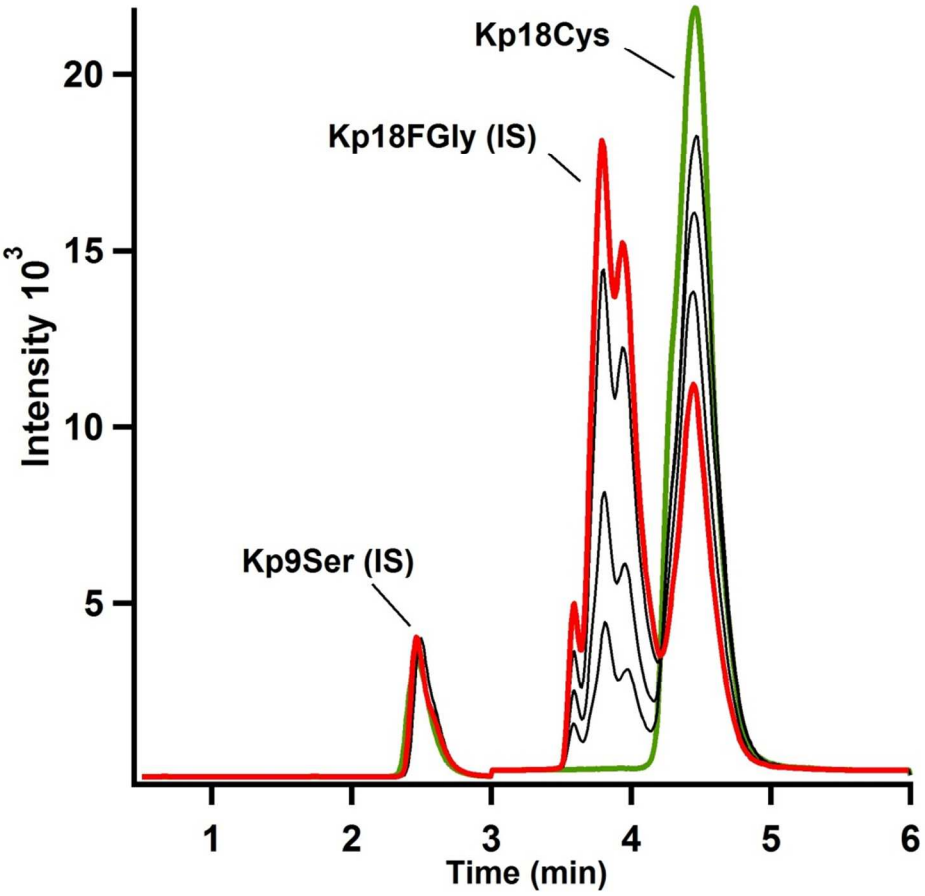
Kp18Cys
Kp18FGly (IS)
Kp9Ser (IS)
Intensity 10^3
20
15
10
5
1
2
3
4
5
6
Time (min)

Figure S4.

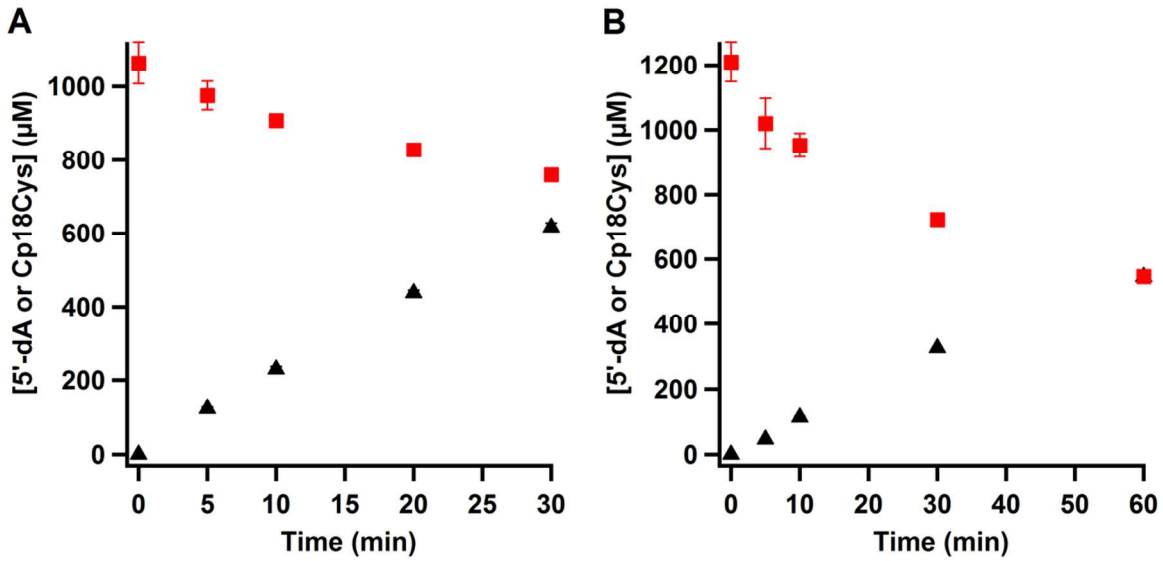
A
[5'-dA or Cp18Cys] (μM)
0
200
400
600
800
1000
0
5
10
15
20
25
30
Time (min)
B
[5'-dA or Cp18Cys] (μM)
0
200
400
600
800
1000
1200
0
10
20
30
40
50
60
Time (min)

Figure S5.

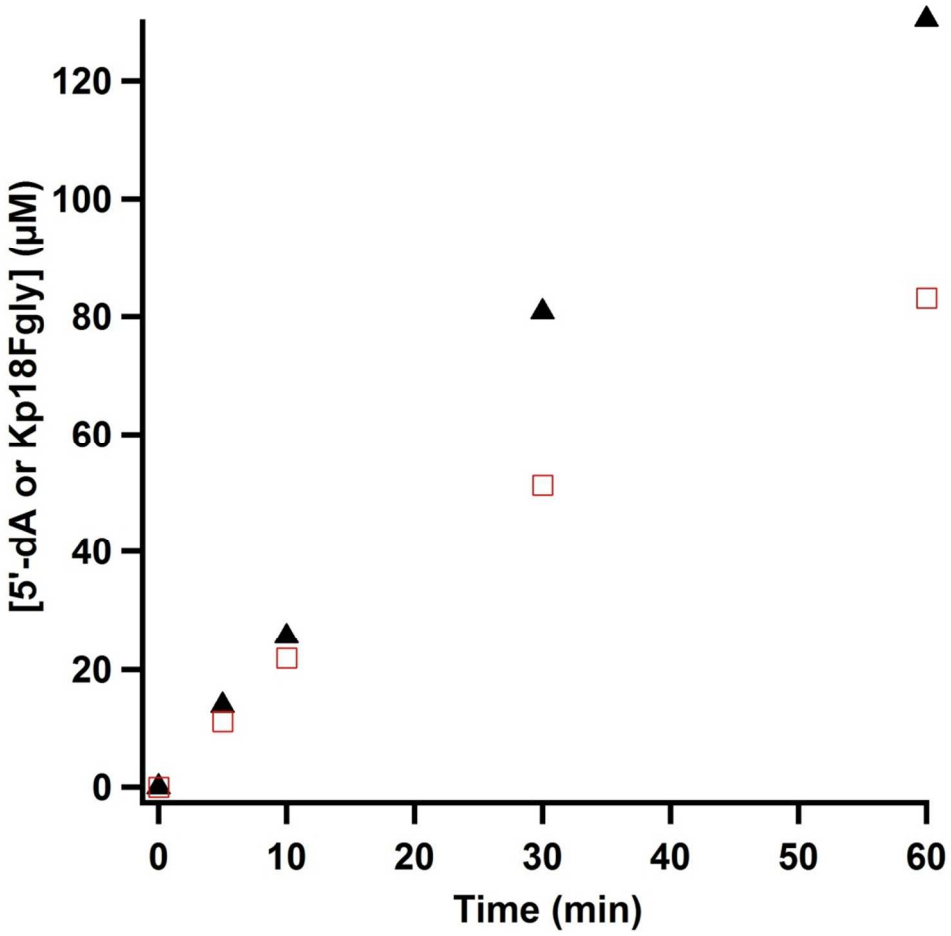
[5'-dA or Kp18Fgly] (μM)
120
100
80
60
40
20
0
0
10
20
30
40
50
60
Time (min)

Figure S6.

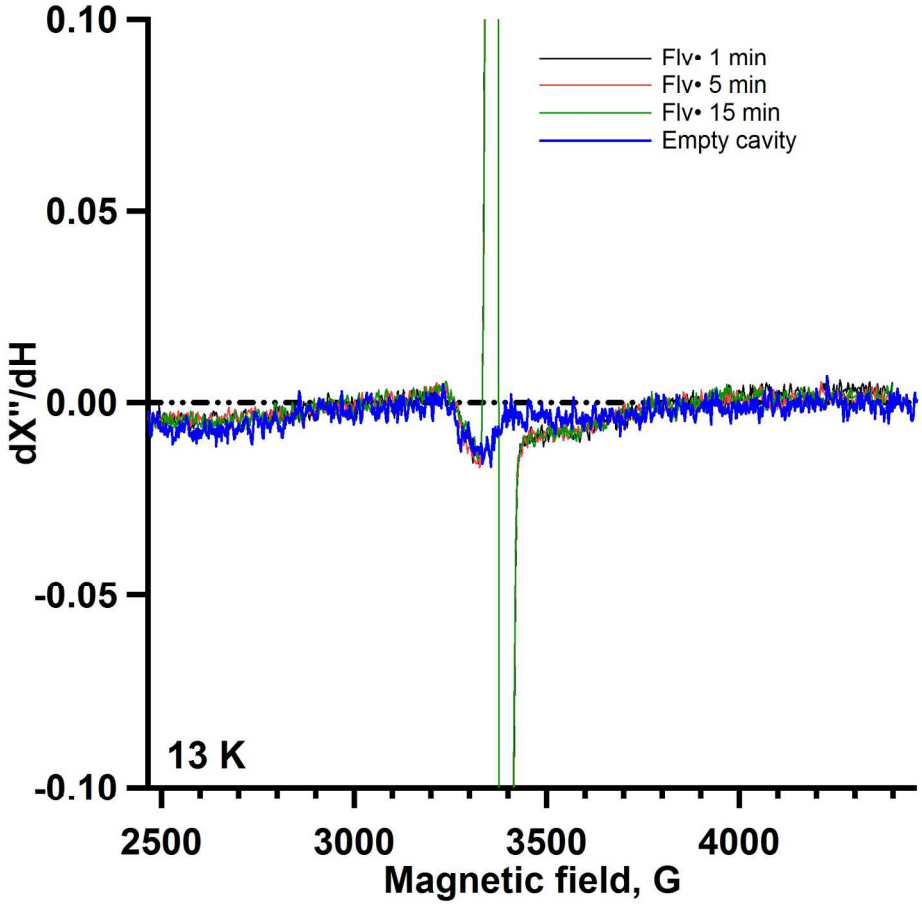
0.10
0.05
0.00
-0.05
-0.10
dX''/dH
13 K
2500
3000
3500
4000
Magnetic field, G
Flv• 1 min
Flv• 5 min
Flv• 15 min
Empty cavity

Figure S7.

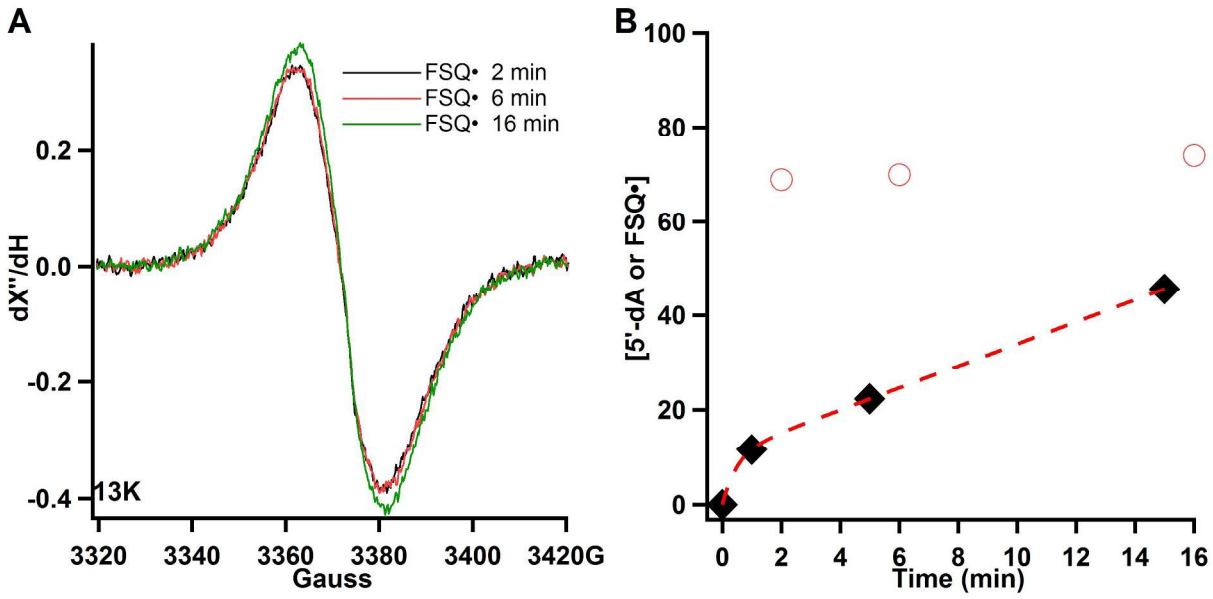
A
FSQ• 2 min
FSQ• 6 min
FSQ• 16 min
dX''/dH
0.2
0.0
-0.2
-0.4
13K
3320
3340
3360
3380
3400
3420G
Gauss
B
100
80
60
40
20
0
[5'-dA or FSQ•]
0
2
4
6
8
10
12
14
16
Time (min)

Figure S8.

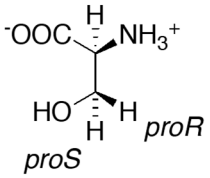

L-serine

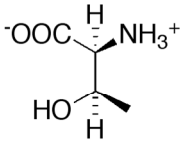

2S,3R

L-threonine

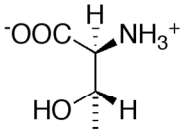

2S,3S

L-*allo*-threonine

Figure S9.

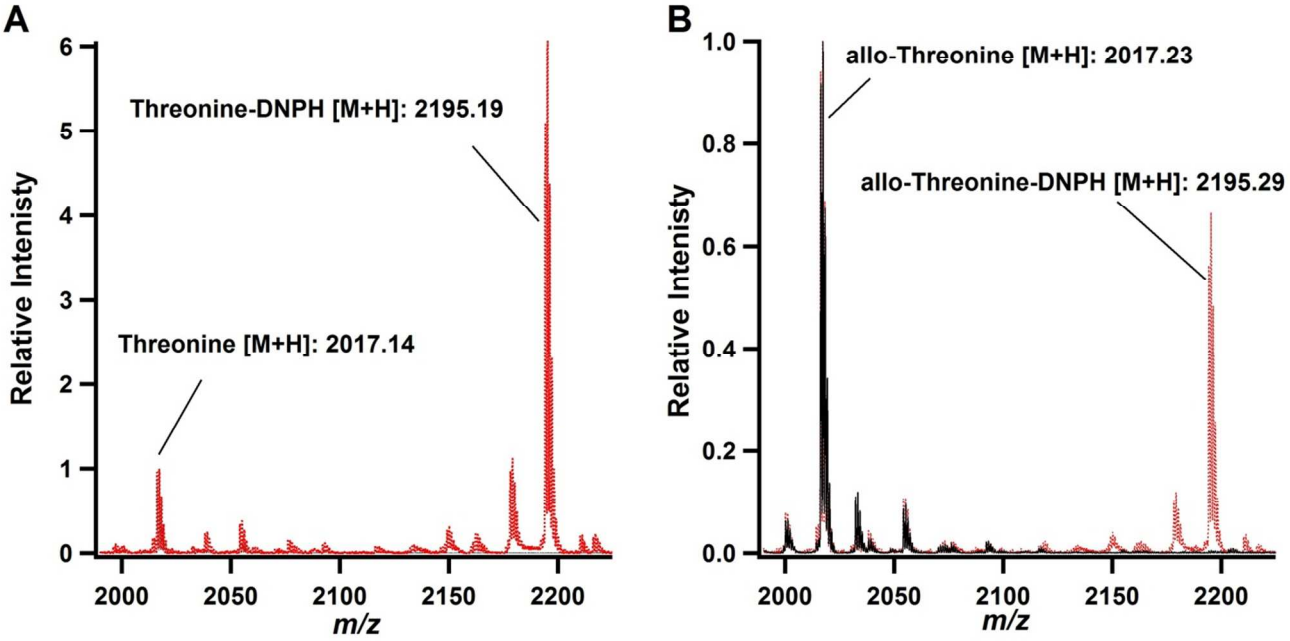
A
Threonine-DNPH [M+H]: 2195.19
Threonine [M+H]: 2017.14
Relative Intenisty
m/z
B
allo-Threonine [M+H]: 2017.23
allo-Threonine-DNPH [M+H]: 2195.29
Relative Intenisty
m/z

Figure S10.

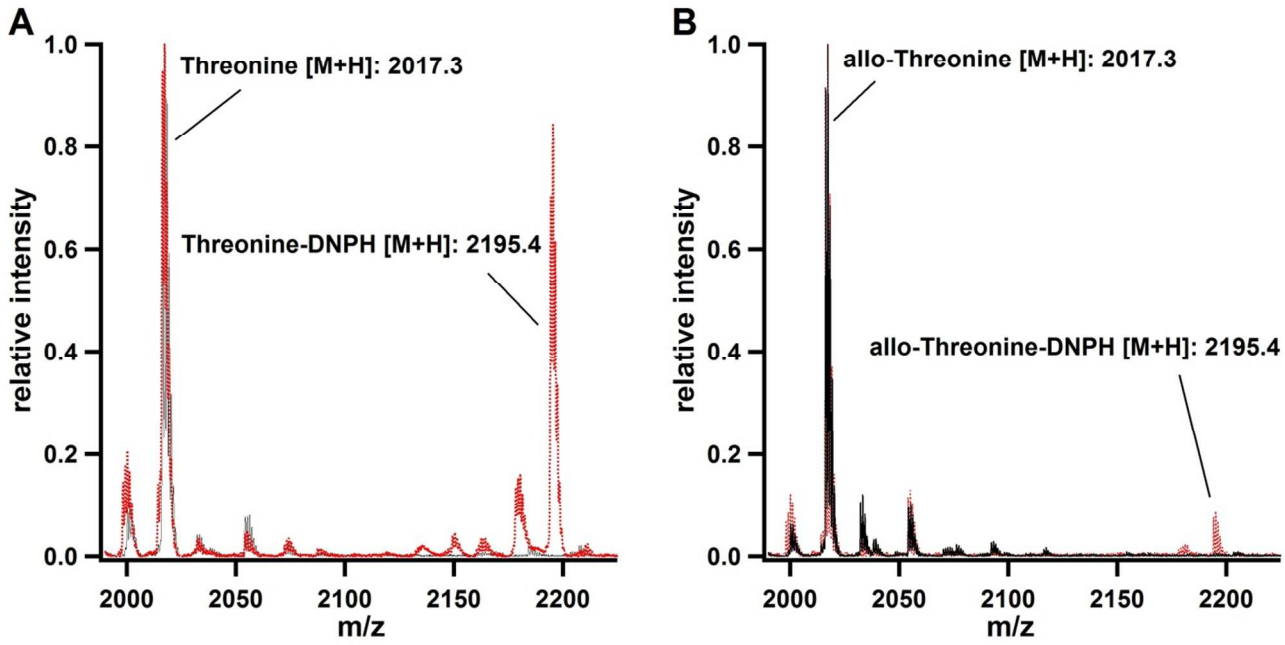
A
1.0
0.8
0.6
0.4
0.2
0.0
relative intensity
Threonine [M+H]: 2017.3
Threonine-DNPH [M+H]: 2195.4
2000
2050
2100
2150
2200
m/z
B
1.0
0.8
0.6
0.4
0.2
0.0
relative intensity
allo-Threonine [M+H]: 2017.3
allo-Threonine-DNPH [M+H]: 2195.4
2000
2050
2100
2150
2200
m/z

Figure S11.

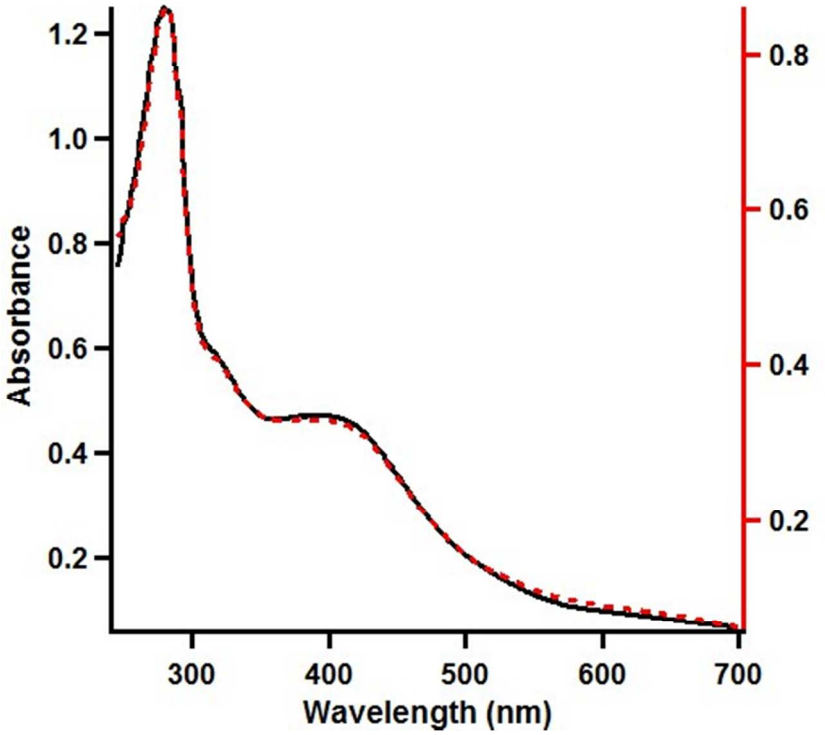
Absorbance
1.2
1.0
0.8
0.6
0.4
0.2
0.8
0.6
0.4
0.2
300
400
500
600
700
Wavelength (nm)

Figure S12.

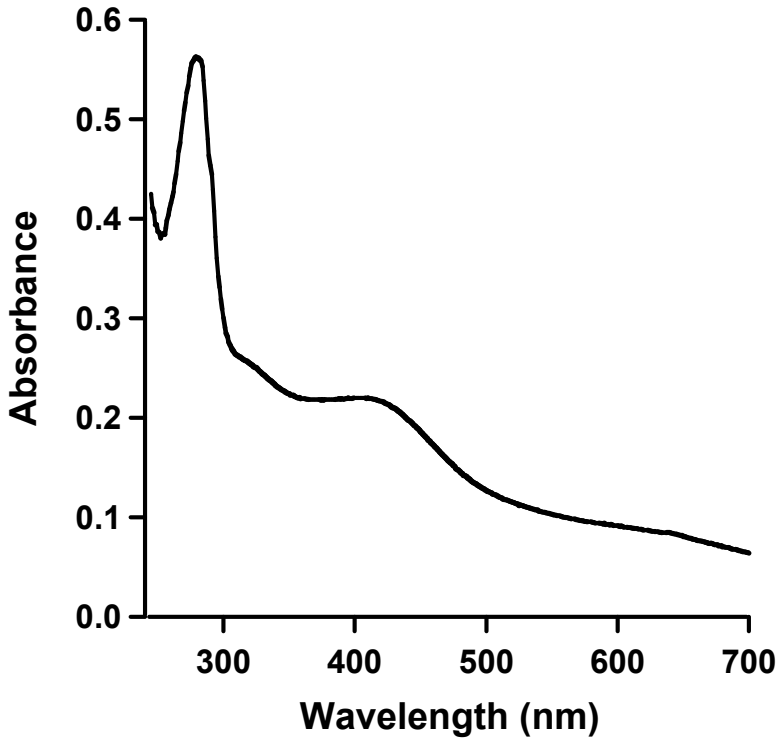
0.6
0.5
0.4
0.3
0.2
0.1
0.0
Absorbance
300
400
500
600
700
Wavelength (nm)

Figure S13

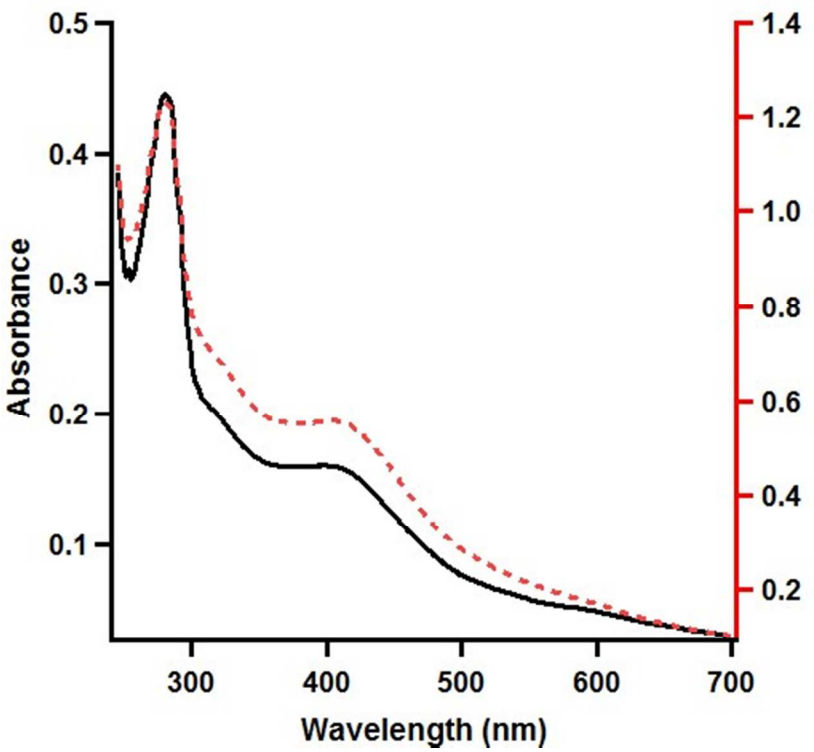
0.5
0.4
0.3
0.2
0.1
Absorbance
1.4
1.2
1.0
0.8
0.6
0.4
0.2
300
400
500
600
700
Wavelength (nm)

Figure S14.

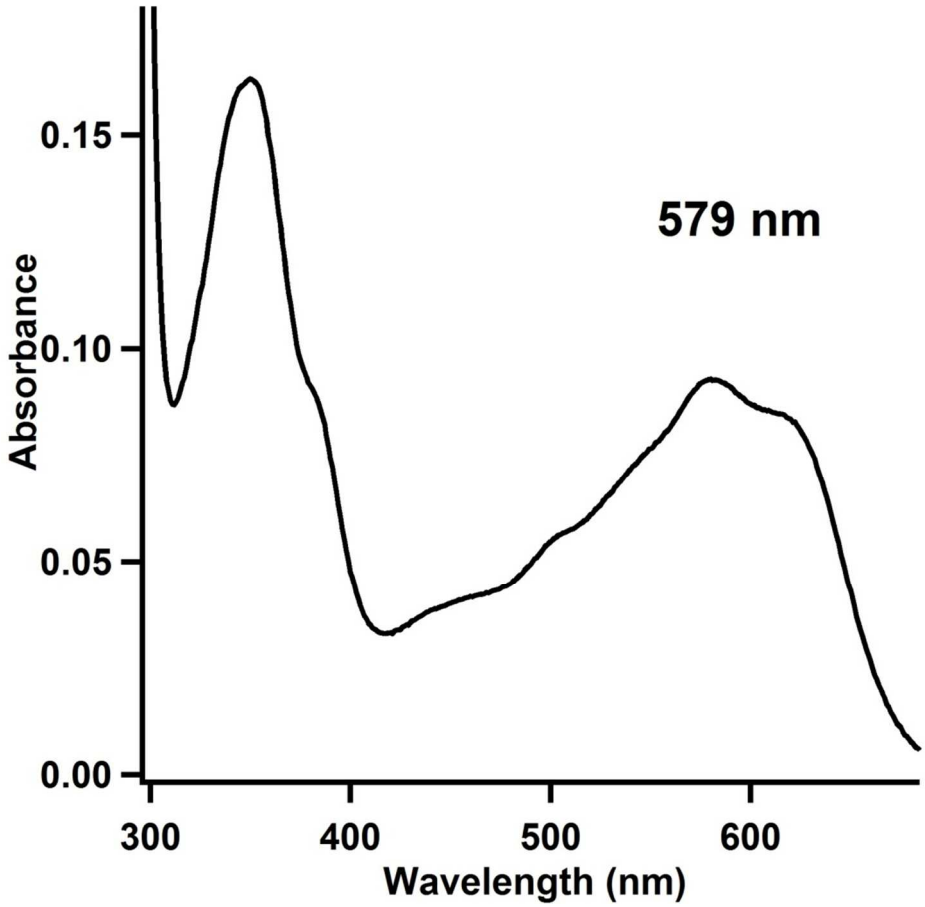
579 nm
Absorbance
0.15
0.10
0.05
0.00
300
400
500
600
Wavelength (nm)

References

1. *Grove, T. L., Lee, K. H., St Clair, J., Krebs, C., and Booker, S. J. (2008) In vitro characterization of AtsB, a radical SAM formylglycine-generating enzyme that contains three [4Fe-4S] clusters, Biochemistry 47, 7523–7538.*